Protein Aggregation Hot Paper

Deutsche Ausgabe: DOI: 10.1002/ange.201606544
Internationale Ausgabe: DOI: 10.1002/anie.201606544

Direct Observation of Aggregation-Induced Backbone Conformational Changes in Tau Peptides

*A. C. Jiji, A. Shine, and Vinesh Vijayan**

Abstract: *In tau proteins, the hexapeptides in the R2 and R3 repeats are known to initiate tau fibril formation, which causes a class of neurodegenerative diseases called the taupathies. We show that in R3, in addition to the presence of the hexapeptides, the correct turn conformation upstream to it is also essential for producing prion-like fibrils that are capable of propagation. A time-dependent NMR aggregation assay of a slow fibril forming R3-S316P peptide revealed a trans to cis equilibrium shift in the peptide-bond conformation preceding P316 during the growth phase of the aggregation process. S316 was identified as the key residue in the turn that confers templating capacity on R3 fibrils to accelerate the aggregation of the R3-S316P peptide. These results on the specific interactions and conformational changes responsible for tau aggregation could prove useful for developing an efficient therapeutic intervention in Alzheimer's disease.*

The abnormal aggregation of tau proteins to form the paired helical filaments (PHFs) that constitute the major part of neurofibrillary tangles (NFTs)[1] is involved in many neuronal diseases, including chronic traumatic encephalopathy (CET)[2] and Alzheimer's disease.[3] Tau proteins are predominantly unfolded in solution and slowly aggregate to form long fibrils that constitute the PHFs.[4] In the different isoforms of tau protein, 3 or 4 repeat domains of around 32 amino acid residues are located at the C-terminal part.[5] Studies with protease digestion as well as fluorescence spectroscopy have revealed that the cores of tau fibrils from different isoforms are made up of the R2 and R3 repeat for the four-repeat isoform and only the R3 repeat in the case of the three-repeat isoform.[6] The R2 and R3 repeats contain a hexapeptide (^{306}VQIVYK^{311}) motif that is known to form fibrils on its own.[7] Mutations in the hexapeptide lead to the abrogation of tau fibril formation.[8] Furthermore, the X-ray structure of the hexapeptides in R3 reveals a steric zipper arrangement consistent with the model of fibril initiation in many of the amyloid proteins.[9] However, from solid-state NMR (ssNMR) studies on tau fibrils, at least two additional β-strand regions in R3, upstream to the hexapeptide, have also been identified to form the core of the fibril.[10] These strands are 1) V313–L315, which is sandwiched between a kink at P312 and the second kink at S316, and 2) K317–K321, which is found after the kink at S316.

Nevertheless, the exact arrangement of β-strands within the monomeric unit of the fibrils was undetermined. Moreover, the structural importance of the kink residues in promoting aggregation is also unknown. This is crucial for understanding the early stages of fibril formation.[11] In this work, we engineered peptides from the fibril-forming core of tau (R3; Figure 1) that encompass the hexapeptide but have different aggregation properties depending on the presence of the key kink residue S316 in the peptide sequence. In the slow fibril forming R3-S316P peptide, we show compelling evidence that a *trans*-to-*cis* conformation shift in the peptide bond preceding P316 occurs during peptide aggregation. We show that seeding of the R3-S316P peptide depends critically on the presence of S316 in the peptide sequence of the templating fibrils, which reveals a structural link between the mutant and the wild-type peptides.

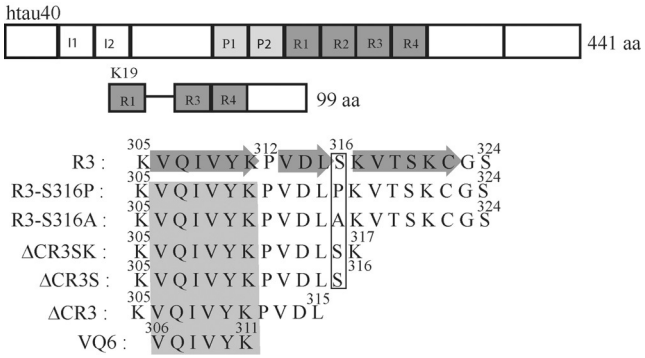

Figure 1. Tau isoforms and the tau-derived peptides used in this study. htau40 is the longest isoform found in the human central nervous system (441 residues), containing two N-terminal inserts and four repeating units (R1, R2, R3, R4). The K19 construct contains three of the four repeats. The peptide sequences used in our study are shown at the bottom. The hexapeptide motif is shaded in all the sequences. The secondary structure from solid-state NMR studies is shaded on the R3 sequence.

The solution conformations of peptides derived from the R3 repeat sequence of tau (Figure 2) were compared (Table S2–S5 in the Supporting Information). The R3 peptide contains the residues that form the non-polymorphic part of the tau fibrils.[10b] Furthermore, R3 is known to self-assemble to form amyloid fibrils even without aggregation-inducing heparin.[12] The other peptides are also from the R3 repeat but contain a subset of R3 peptide sequences with varying peptide chain length but with the hexapeptide fragment in their amino

[*] A. C. Jiji, A. Shine, Dr. V. Vijayan
School of Chemistry, Indian Institute of Science Education and Research Thiruvananthapuram (IISER-TVM)
CET campus, Trivandrum-695016 (India)
E-mail: vinesh@iisertvm.ac.in

Supporting information for this article can be found under: http://dx.doi.org/10.1002/anie.201606544.

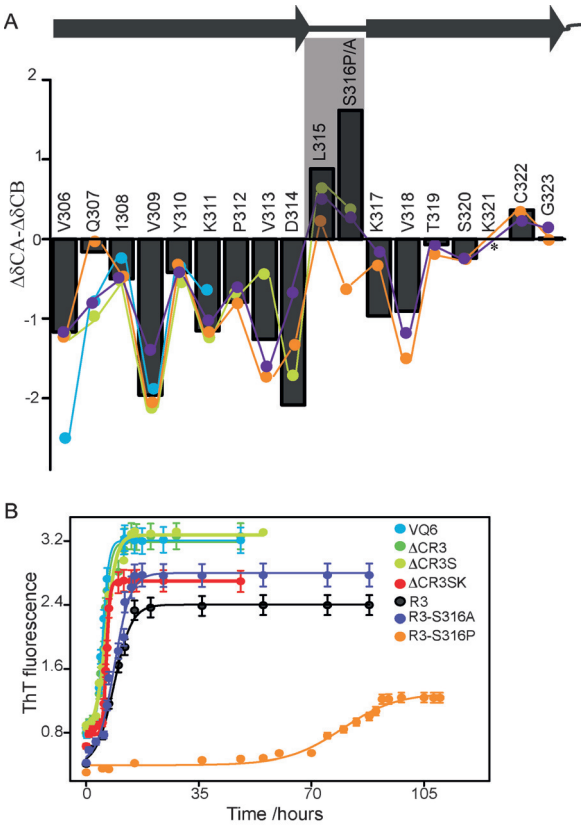

Figure 2. A) Secondary chemical shift (SCS) analysis of R3 (shaded bars), R3-S316P (orange lines), R3-S316A (purple lines), ΔCR3S (yellow lines), VQ6 (blue lines) tau peptides. Successive negative values indicate a β-strand conformation. Note the break in the β-strand between D314 and K317 in R3. ΔCR3S and R3-S316A also show positive a SCS for L315 and S316 in analogy to R3. R3-S316P shows negative SCS for P316. The hexapeptide VQ6 shows an extended β-strand conformation and the secondary structure of this region is conserved in all of the peptide constructs of R3. The secondary structure propensity of R3 is depicted at the top of the graph. B) Kinetic profile for a ThT aggregation assay of the VQ6, ΔCR3, ΔCR3S, ΔCR3SK, R3, R3-S316P, and R3-S316A peptides.

acid chain. The negative secondary chemical shift (SCS) for most residues in these peptides denotes β-strand propensity. Residues L315 and S316 of R3 peptides with positive SCS values are the only significant exceptions to the observed β-strand propensity (Figure 2, shaded region). The SCS of the R3 peptide matches the SCS of corresponding residues of the longer construct K18 tau (BMRB ID 19253, Figure S12 in the Supporting Information).[13] A type 1 β-turn motif encompassing the ^{315}LS^{316} residues (^{314}DLSK^{317}) has previously been proposed for full-length tau in solution.[14] The characteristic non-β dihedral for the middle two (LS) residues is typical for a type 1 β-turn. Interestingly, the general SCS trend for R3 peptides (in solution) is similar to the SCS pattern observed for K19 fibrils (Figure S13). The similarity between the SCS values of R3 in solution and in fibrils suggests that the majority of the peptide in solution is in the fibril-forming conformation. Even in the ^{315}LS^{316} region, where relative differences in SCS are observed, S316 adopts a non-β dihedral angle to produce a kink in the β-strands of the fibril.[10b]

A proline mutation at position 316 of R3 was prepared in order to investigate how the structural and kinetic properties of the peptide alter the nature of the second kink residue of the fibril. The change from serine to a proline was intended to restrict the dihedral angle space at position 316 of the amino acid sequence.[15] The motional restriction of the pyrrolidine ring in proline allows it to act as a turn inducer. The replacement of the kink-inducing serine with a proline should thus be structurally compatible with the fibrils. The SCS of the resulting R3-S316P peptide shows similar β-strand propensity to R3. Even though P316 shows a negative SCS, the lack of an alpha amino hydrogen atom precludes proline incorporation into a β-sheet conformation. R3 peptide with an alanine mutation at position 316 was also prepared (R3-S316A). Analogous to R3-S316P, R3-S316A replaces a polar residue with a hydrophobic residue. However unlike the proline, there is no dihedral restriction in alanine. The SCS of the ^{315}LA^{316} region of the peptide matches with that of R3, thus establishing that the β-turn region is conserved in the mutant peptides. Hence, in both mutants, the change in the primary structure did not alter the β-turn propensity.

Remarkably, all of the peptides that were prepared formed fibrils. However, their structure morphology and aggregation kinetics differed (Figure 2B, Figures S15, S17). The aggregation kinetics of the different peptides were followed by monitoring the increase in the fluorescence intensity of Thioflavin T (ThT) (Figure 2B). The lag time, which indicates how slow aggregation is, was determined by using a nonlinear fit of the ThT aggregation profile using a nucleation–polymerization model.[16] The hexapeptide and other shorter constructs form fibrils without any substantial lag time (4 hours, Figure 2B, green to red). An AFM image of fibrils formed by the shorter peptides showed plenty of short fibrils (Figure S15D, E). In addition to the short fibrils, a small number of longer fibrils were found for ΔCR3SK (Figure S15F).[17] The measured lag time for R3 (10 hours) is comparable to the previously known value for K19.[18] The R3-S316A peptide aggregates at a very similar rate (Figure 2B), producing high-density of fibrils in AFM (Figure S17A). Strikingly, the R3-S316P peptide shows a considerable lag time for fibril formation (ca. 70 hours). The lag times measured for different concentrations of R3-S316P were approximately eight-fold longer than those observed for the corresponding concentrations of R3 peptide (Figure S16A, B). Compared to the R3 peptide, the ThT intensity at the end of aggregation of the R3-S316P peptide was lower, thus suggesting the formation of a lower concentration of fibrils (Figure 2B). Consequently, the AFM images of R3-S316P show less-dense fibrils than R3 (Figure 15A–C and Figure S17B). From the UV absorbance measurements of the dissolved peptides, we found that around 42% of the initial R3-S316P peptide remains in solution compared to only 8.3% for R3 (Figure S18) after the end of aggregation. Less than half of R3-S316P peptide remains in solution at the end of aggregation. Despite the similar structural propensities, the proline mutation of the second kink residue in R3 results in a notable difference in the aggregation properties of the peptide.

To monitor possible structural changes associated with aggregation of the putative kink residues (P312 and P316) in R3-S316P fibrils, ^{13}C-labeled P312 R3-S316P (^{13}C-P312-R3-S316P) and ^{13}C-labeled P312, P316 R3-S316P (^{13}C-P312,P316-R3-S316P) peptides were prepared. After the addition of heparin, ^{13}C-^{1}H-HSQC experiments were performed at regular intervals to give an NMR aggregation assay of both peptides. A ThT assay was also carried out simultaneously on duplicate samples. The peaks corresponding to the *cis*/*trans* form of the proline were clearly visible in the HSQCs. During the NMR aggregation assay, no chemical-shift changes were observed. In the case of the ^{13}C-P312-R3-S316P samples, no intensity change in the signals was noted. The native P312 in R3-S316P remained in *trans* configuration during the entire aggregation process (96%). However for the ^{13}C-P312,P316-R3-S316P peptide, the NMR signal intensity corresponding to the *cis* and *trans* forms of the proline changed during aggregation. From about 94 hours into aggregation, the signal intensity corresponding to the *cis* proline started increasing, with a corresponding decrease in the signal intensity for the *trans* conformation. Since the P312 remains in the *trans* configuration, there is clearly a *trans*-to-*cis* equilibrium shift in the P316 configuration upon peptide aggregation. At saturation point, the population of the *cis* peptide bond reached nearly 42%, with a 30% decrease in *trans* configuration.

Interestingly, the time-dependent fluorescence intensity variation shown by ThT and the NMR peak intensity variation for *cis*-P316 are similar. Similar kinetic profiles from the ThT assay and *cis*-P316 formation show that the aggregation process and *cis*-P316 formation are coupled. Consequently, the increase in the *cis*-P316 intensity can be fitted to a nucleation–polymerization aggregation model to provide a rate constant and lag time ($k = 0.131\ h^{-1}$ lag time = 94 h) that are comparable with those obtained from the ThT kinetic profile ($k = 0.124\ h^{-1}$, lag time = 106 h). During the growth phase, a substantial increase in NMR line width was specifically observed for *cis*-proline peaks (Figure S19). The line width increase is likely a result of accelerated formation of oligomers. Differential line broadening confirms that *cis*-P316 is the only conformer involved in oligomer formation. The relatively faster kinetics of *cis*-P316 formation indicate the soluble oligomer formation that precedes fibril formation, as reported by the ThT assay (Figure S20). Correlating with the conversion of soluble monomers/oligomers into insoluble fibrils, a reduction in the NMR signal intensity of the *cis* and *trans* forms of proline is clearly observed near the end of aggregation (ca. 130 hours, Figure 3C). Notably, a decrease in NMR peak intensity is observed as the ThT fluorescence reaches saturation (Figure S20). Interestingly, a recent study on tau has shown that the aggregation proceeds via monomeric assembly into small oligomers, which then undergo slow structural conversion before fibril formation.[19]

The change in the equilibrium constant for the *cis*–*trans* isomerism of the leucine–proline peptide bond is associated with a change in ΔG of around -1 kcal mol^{-1} ($\Delta\Delta G$). The long lag time before the exponential increase in the NMR peak intensity for *cis*-P316 and the ThT fluorescence intensity is due to a delay in the formation of a critical nucleus size that

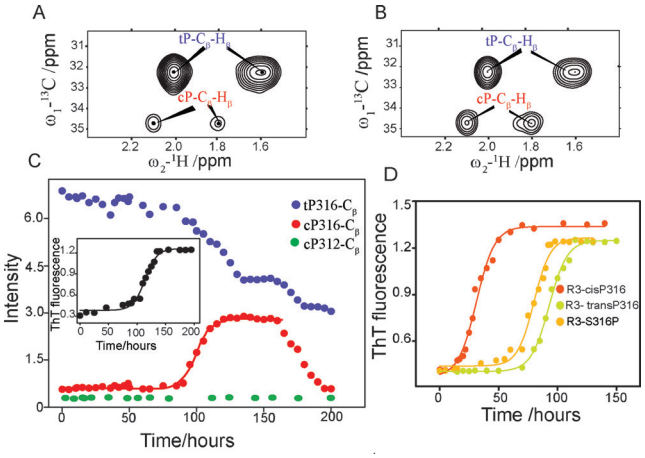

Figure 3. Time-dependent ^{13}C-^{1}H HSQC spectra of R3-S316P with ^{13}C-labeled proline. The peptide concentration was 1 mM and measurements were made at 298 K without sample shaking. The C_β resonances of *trans* and *cis* proline immediately after heparin addition (A) and at 90 hours (B). C) Time variation of C_β intensities of *cis* and *trans* proline in R3-S316P (with ^{13}C and ^{15}N labeled P316 and P312). The measurements were done at regular intervals. C_β intensity for *cis*-P316 (^{13}C-P312,P316-R3-S316P, red filled dots) increased with time while the intensity for *cis*-P312 (^{13}C-P312-R3-S316P, green filled dots) remained invariant. The inset shows ThT kinetic experiment that was performed simultaneously with NMR measurements under identical experimental condition. D) ThT aggregation assay of 50 μM R3-*cis*-P316, R3-*trans*-P316, and R3-S316P at 310 K with shaking. The *cis*-bond-favoring R3-*cis*-P316 aggregate within 30 hours of heparin addition, compared to the normal R3-S316P, which aggregate in around 75 hours. The *trans*-favoring R3-*trans*-P316 aggregates even slower, in around 93 hours.

depends on the initial concentration of the peptide in the *cis* conformation. The nuclei thus formed can catalyze the transformation of *trans*-P316 to *cis*-P316 and thus produce an exponential increase in the percentage of *cis*-P316.[19] In order to confirm our results, we synthesized two different peptides wherein (2*S*,4*S*)-fluoroproline (R3-*cis*-P316) or the stereoisomeric (2*S*,4*R*)-fluoroproline (R3-*trans*-P316) replaces P316 in R3-S316P peptide. Compared to normal proline, the (2*S*,4*S*)-fluoroproline is twice as likely to favor the *cis* conformation, while the stereoisomeric (2*S*,4*R*)-fluoroproline favors the *trans* conformation.[20] The aggregation kinetics of R3-*cis*-P316 and R3-*trans*-P316 were followed by ThT assay. As expected, R3-*cis*-P316P aggregates twice as fast (30 hours) while R3-*trans*-P316P aggregates at an even slower rate (93 hours) than regular R3-S316P (75 hours). The lag time is halved for the *cis*-favoring peptide while it increased for the *trans*-favoring peptide. Hence our results clearly show that favoring the *cis* peptide bond of L315-P316 promotes the aggregation of R3-S316P and confirms the time-dependent HSQC data for R3-S316P. *Cis* prolines are usually found in β-turns where a sharp change in direction of β-strands are required.[21] Hence it is likely that a putative type 1 β-turn comprising the ^{314}DLPK^{317} fragment in R3-S316P monomer is changed to a type VI turn (with a *cis* peptide) in the fibrils.

Measuring the seeding properties of tau fibrils is an important approach for checking the structural compatibility and fibril propagation ability of the peptide.[22] The long lag

time of the R3-S316P peptide facilitates seeding experiments, where a significant difference in lag time can be measured easily. The seeds are small fibril fragments obtained from the mature fibrils (see the Supporting Information for details of preparation, Figure S23), which form a growth template for the monomers, thereby resulting in a reduction in the lag phase for the aggregating monomers.[23] The templating effect of the seed is structure-dependent since there has to be equivalence in structure between the seed and the monomer for the templating to be successful.[24] Knowing the seeding efficiency of VQ6, ΔCR3, ΔCR3S, ΔCR3SK, R3, and R3-S316A fibrils on the aggregation of R3-S316P (Figure 4A)

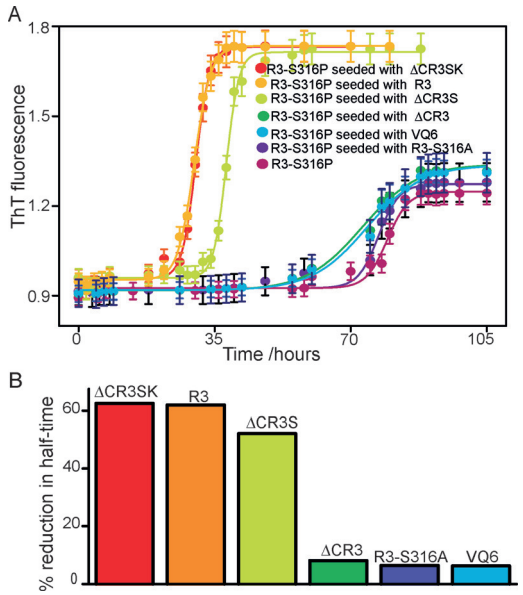

Figure 4. D) Kinetic profile of seeding experiments on R3-S316P monomers using VQ6, ΔCR3, ΔCR3S, ΔCR3SK, R3-S316A, and R3 fibrils. 3 mol% of seed fibrils were used. R3-S316P seeded with ΔCR3S, ΔCR3SK, and R3 showed an increase in ThT intensity accompanied by a shortened lag-time. B) Percentage reduction of half-time (lag-time) of R3-S316P aggregation upon the addition of different peptide fibrils. ΔCR3SK, ΔCR3S, and R3 fibrils reduce the lag times significantly.

peptide should help in accurately evaluating the structural importance of the β-turn sequence in the formation of the fibrils. Among the six peptides, VQ6, ΔCR3, and R3-S316A lack S316 in their peptide sequence. The fibril seeds of these peptides fail to shorten the lag time of R3-S316P aggregation (Figure 4B green, purple, and blue bars). On the other hand, about a 60% reduction in lag time was observed when fibril seeds of ΔCR3S, ΔCR3SK, and R3 were used to seed the aggregation of S316P monomers (Figure 4B red, orange, and pale green bars). The templating ability of R3, ΔCR3S, and ΔCR3SK fibrils to seed the fibril formation of R3-S316P and the inability of R3-S316A to seed R3-S316P fibrils reveal that the structure of wild-type fibrils and R3-S316P fibrils are similar and dissimilar to R3-S316A, respectively. Strikingly, the hydroxy group of S316 clearly influences the propagation ability of fibrils. In the NOESY NMR spectrum of R3, H_β of S316 has a cross-peak with the side chain $H_{N\zeta}$ of a Lysine (Figure S24), thus suggesting a hydrogen bond between the hydroxy group and the amine side chain. The hydrogen bond restricts the conformational freedom of the serine side chain, thereby promoting a particular type of aggregation. Such side-chain interactions were absent in the solution NMR of R3-S316A peptide (Figure S24). Since there is no conformational restriction for the alanine side chain, the aggregation proceeds to give a fibrillar topology different from R3 fibrils.

Our results reveal that in addition to the hexapeptide sequence, the conformation of S316 in the β-turn is crucial for the assembly of long fibrils and provides the prion-like propagation seen in tau proteins.[25] The templating studies show that despite the presence of the hexapeptide in the sequence, fibrils without the S316 residue are unable to seed fibril formation of the R3-S316P mutant. Hence the correct turn conformation is critical for the hexapeptide zipper-like mechanism to efficiently propagate fibril formation. Time-dependent changes in NMR peak intensity during R3-S316P peptide aggregation show that *cis*-P316 conformation is clearly favored for fibril formation. Considering that the fibril seeds of wild-type R3 can seed R3-S316P aggregation, the ^{314}DLSK^{317} β-turn in the monomer of R3 must be converted into a type VI compatible turn in the fibril. It is, therefore, necessary to determine the configuration of serine in the β-turn (kink), since its side-chain orientation and peptide conformation play a crucial role in tau aggregation to produce prion-like propagating fibrils.

Acknowledgements

The authors thank Dr. Mahesh Hariharan and Dr. T. Shyamala for critical reading of the manuscript, Shine K. Albert for help with AFM studies, RGCB Trivandrum for MALDI, University of Madras for TEM studies. Jiji thanks CSIR-JRF for PhD grant and V.V. thanks IISER Thiruvananthapuram and SERB (EMR/2015/000111) for funding.

Keywords: Alzheimer's disease · fibrillation · *cis*–*trans* isomerism · NMR spectroscopy · peptides

How to cite: *Angew. Chem. Int. Ed.* **2016**, *55*, 11562–11566
Angew. Chem. **2016**, *128*, 11734–11738

[1] V. M. Y. Lee, B. J. Balin, L. Otvos, J. Q. Trojanowski, *Science* **1991**, *251*, 675–678.
[2] K. Blennow, J. Hardy, H. Zetterberg, *Neuron* **2012**, *76*, 886–899.
[3] a) V. M. Y. Lee, M. Goedert, J. Q. Trojanowski, *Annu. Rev. Neurosci.* **2001**, *24*, 1121–1159; b) L. I. Binder, A. L. Guillozet-Bongaarts, F. Garcia-Sierra, R. W. Berry, *Biochim. Biophys. Acta Mol. Basis Dis.* **2005**, *1739*, 216–223; c) K. Iqbal, A. D. C. Alonso, S. Chen, M. O. Chohan, E. El-Akkad, C. X. Gong, S. Khatoon, B. Li, F. Liu, A. Rahman, H. Tanimukai, I. Grundke-Iqbal, *Biochim. Biophys. Acta Mol. Basis Dis.* **2005**, *1739*, 198–210.
[4] a) M. Goedert, R. Jakes, M. G. Spillantini, M. Hasegawa, M. J. Smith, R. A. Crowther, *Nature* **1996**, *383*, 550–553; b) P. Friedhoff, M. von Bergen, E.-M. Mandelkow, P. Davies, E. Mandelkow, *Proc. Natl. Acad. Sci. USA* **1998**, *95*, 15712–15717; c) D. W. Cleveland, S. Y. Hwo, M. W. Kirschner, *J. Mol. Biol.* **1977**, *116*, 227–247.

[5] a) M. Goedert, C. M. Wischik, R. A. Crowther, J. E. Walker, A. Klug, *Proc. Natl. Acad. Sci. USA* **1988**, *85*, 4051 – 4055; b) B. Trinczek, J. Biernat, K. Baumann, E. M. Mandelkow, E. Mandelkow, *Mol. Biol. Cell* **1995**, *6*, 222.

[6] a) L. Li, M. von Bergen, E.-M. Mandelkow, E. Mandelkow, *J. Biol. Chem.* **2002**, *277*, 41390 – 41400; b) M. von Bergen, S. Barghorn, S. A. Muller, M. Pickhardt, J. Biernat, E. M. Mandelkow, P. Davies, U. Aebi, E. Mandelkow, *Biochemistry* **2006**, *45*, 6446 – 6457; c) K. Tomoo, T.-M. Yao, K. Minoura, S. Hiraoka, M. Sumida, T. Taniguchi, T. Ishida, *J. Biochem.* **2005**, *138*, 413 – 423.

[7] M. von Bergen, S. Barghorn, L. Li, A. Marx, J. Biernat, E. M. Mandelkow, E. Mandelkow, *J. Biol. Chem.* **2001**, *276*, 48165 – 48174.

[8] a) W. J. Goux, L. Kopplin, A. D. Nguyen, K. Leak, M. Rutkofsky, V. D. Shanmuganandam, D. Sharma, H. Inouye, D. A. Kirschner, *J. Biol. Chem.* **2004**, *279*, 26868 – 26875; b) M. von Bergen, P. Friedhoff, J. Biernat, J. Heberle, E. M. Mandelkow, E. Mandelkow, *Proc. Natl. Acad. Sci. USA* **2000**, *97*, 5129 – 5134; c) S. R. Meng, Y. Z. Zhu, T. Guo, X. L. Liu, J. Chen, Y. Liang, *PLoS One* **2012**, *7*, e38903.

[9] M. R. Sawaya, S. Sambashivan, R. Nelson, M. I. Ivanova, S. A. Sievers, M. I. Apostol, M. J. Thompson, M. Balbirnie, J. J. W. Wiltzius, H. T. McFarlane, A. O. Madsen, C. Riekel, D. Eisenberg, *Nature* **2007**, *447*, 453 – 457.

[10] a) O. C. Andronesi, M. von Bergen, J. Biernat, K. Seidel, C. Griesinger, E. Mandelkow, M. Baldus, *J. Am. Chem. Soc.* **2008**, *130*, 5922 – 5928; b) V. Daebel, S. Chinnathambi, J. Biernat, M. Schwalbe, B. Habenstein, A. Loquet, E. Akoury, K. Tepper, H. Muller, M. Baldus, C. Griesinger, M. Zweckstetter, E. Mandelkow, V. Vijayan, A. Lange, *J. Am. Chem. Soc.* **2012**, *134*, 13982 – 13989.

[11] a) T. Eichner, A. P. Kalverda, G. S. Thompson, S. W. Homans, S. E. Radford, *Mol. Cell* **2011**, *41*, 161 – 172; b) F. Chiti, C. M. Dobson, *Nat. Chem. Biol.* **2009**, *5*, 15 – 22.

[12] J. Adamcik, A. Sanchez-Ferrer, N. Ait-Bouziad, N. P. Reynolds, H. A. Lashuel, R. Mezzenga, *Angew. Chem. Int. Ed.* **2016**, *55*, 618 – 622; *Angew. Chem.* **2016**, *128*, 628 – 632.

[13] S. Wegmann, I. D. Medalsy, E. Mandelkow, D. J. Muller, *Proc. Natl. Acad. Sci. USA* **2013**, *110*, E313 – E321.

[14] M. D. Mukrasch, P. Markwick, J. Biernat, M. von Bergen, P. Bernado, C. Griesinger, E. Mandelkow, M. Zweckstetter, M. Blackledge, *J. Am. Chem. Soc.* **2007**, *129*, 5235 – 5243.

[15] a) E. G. Hutchinson, J. M. Thornton, *Protein Sci.* **1994**, *3*, 2207 – 2216; b) K. Guruprasad, S. Rajkumar, *J. Biosci.* **2000**, *25*, 143 – 156; c) D. Q. McDonald, W. C. Still, *J. Org. Chem.* **1996**, *61*, 1385 – 1391.

[16] M. S. Celej, E. A. Jares-Erijman, T. M. Jovin, *Biophys. J.* **2008**, *94*, 4867 – 4879.

[17] P. Ganguly, T. D. Do, L. Larini, N. E. LaPointe, A. J. Sercel, M. F. Shade, S. C. Feinstein, M. T. Bowers, J. E. Shea, *J. Phys. Chem. B* **2015**, *119*, 4582 – 4593.

[18] S. Jeganathan, M. von Bergen, E. M. Mandelkow, E. Mandelkow, *Biochemistry* **2008**, *47*, 10526 – 10539.

[19] S. I. Cohen, S. Linse, L. M. Luheshi, E. Hellstrand, D. A. White, L. Rajah, D. E. Otzen, M. Vendruscolo, C. M. Dobson, T. P. Knowles, *Proc. Natl. Acad. Sci. USA* **2013**, *110*, 9758 – 9763.

[20] a) C. Renner, S. Alefelder, J. H. Bae, N. Budisa, R. Huber, L. Moroder, *Angew. Chem. Int. Ed.* **2001**, *40*, 923 – 925; *Angew. Chem.* **2001**, *113*, 949 – 951; b) V. Y. Torbeev, D. Hilvert, *Proc. Natl. Acad. Sci. USA* **2013**, *110*, 20051 – 20056.

[21] P. N. Lewis, F. A. Momany, H. A. Scheraga, *Biochim. Biophys. Acta Protein Struct.* **1973**, *303*, 211 – 229.

[22] V. Meyer, P. D. Dinkel, Y. Luo, X. Yu, G. Wei, J. Zheng, G. R. Eaton, B. Ma, R. Nussinov, S. S. Eaton, M. Margittai, *Angew. Chem. Int. Ed.* **2014**, *53*, 1590 – 1593; *Angew. Chem.* **2014**, *126*, 1616 – 1619.

[23] a) J. T. Jarrett, P. T. Lansbury, Jr., *Biochemistry* **1992**, *31*, 12345 – 12352; b) J. D. Harper, P. T. Lansbury, Jr., *Annu. Rev. Biochem.* **1997**, *66*, 385 – 407.

[24] a) P. Chien, J. S. Weissman, A. H. DePace, *Annu. Rev. Biochem.* **2004**, *73*, 617 – 656; b) A. Sidhu, I. Segers-Nolten, V. Subramaniam, *ACS Chem. Neurosci.* **2016**, *7*, 719.

[25] a) P. Brundin, R. Melki, R. Kopito, *Nat. Rev. Mol. Cell Biol.* **2010**, *11*, 301 – 307; b) D. W. Sanders, S. K. Kaufman, S. L. DeVos, A. M. Sharma, H. Mirbaha, A. Li, S. J. Barker, A. C. Foley, J. R. Thorpe, L. C. Serpell, T. M. Miller, L. T. Grinberg, W. W. Seeley, M. I. Diamond, *Neuron* **2014**, *82*, 1271 – 1288; c) A. Siddiqua, Y. Luo, V. Meyer, M. A. Swanson, X. Yu, G. Wei, J. Zheng, G. R. Eaton, B. Ma, R. Nussinov, S. S. Eaton, M. Margittai, *J. Am. Chem. Soc.* **2012**, *134*, 10271 – 10278.

Received: July 6, 2016
Published online: August 11, 2016

